

## Numerical Analysis of heat transfer in a channel Wit in clined baffles

M.A. Louhibi<sup>1</sup>, N. Salhi<sup>1</sup>, H. Bouali<sup>2</sup>, K. Amghar<sup>1</sup>

<sup>1</sup>Laboratoire de Mécanique et Energétique, 1 Faculté des Sciences, BP. 717 Boulevard Mohamed  
VI - 60000 Oujda, Maroc

<sup>2</sup>Ecole supérieure de technologie, Oujda, Maroc

---

**ABSTRACT:** This is a numerical analysis of, forced convection heat transfer inside a channel of rectangular section, containing some inclined baffle plates. We have used a numerical model based on a finite-volume method, and The SIMPLE algorithm [6] was adopted to solve the coupling pressure-velocity problem. Effects of various parameters of the baffles, such as, baffle's inclination angle for two cases 'channel with one or two baffles' on isotherms, streamlines, temperatures distributions and Nusselt number values was studied. It is concluded that baffles angle inclination has a meaningful effect on isotherms, streamlines and total heat transfer through the channel. Indeed, the increase in the baffle inclination improves heat transfer within the channel. Also, heat transfer becomes decreasingly important with adding baffles.

**KEYWORDS:** Forced Convection, Inclined Baffles, Finite Volume Method, SIMPLE, Quick,  $k-\varepsilon$

---

### I. INTRODUCTION:

Turbulent forced convection in heat exchangers with different type of baffles was investigated, recently, in a large number of experimental and numerical works [1-4]. This interest is due to the various industrial applications of this type of configuration such as cooling of nuclear power plants and aircraft engine ... etc. S. V Patankar and EM Sparrow [1] solved numerically the problem of fluid flow and heat transfer in fully developed heat exchangers. These one was equipped by isothermal plate placed transversely to the direction of flow. They found solid plates caused strong recirculation zones in the flow field. They concluded that the Nusselt number depends strongly on the Reynolds number, and it is higher in the case of fully developed then that of laminar flow regime.

Demartini et al [2] conducted numerical and experimental investigations on turbulent flow inside a rectangular channel containing two rectangular baffles. They found that numerical results were in good agreement with those obtained by experiment. In conclusion, baffles play an important role in the dynamic exchangers studied. Indeed, regions of high pressure 'recirculation regions' are formed nearly to chicanes.

Recently, Nasiruddin and Siddiqui [3] studied numerically effects of baffles on forced convection flow in a heat exchanger. The effects of size and inclination angle of baffles were detailed. They considered three different arrangements of baffles. They found that increasing the size of the vertical baffle substantially improves the Nusselt number. However, the pressure loss is also important. For the case of inclined baffles, they found that the Nusselt number is maximum for angles of inclination directed downstream of the baffle, with a minimum of pressure loss.

More recently, Saim et al [4] presented a numerical study of the dynamic behavior of turbulent air flow in horizontal channel with transverse baffles. They adapted numerical finite volume method based on the SIMPLE algorithm and chose  $k-\varepsilon$  model for treatment of turbulence. Results obtained for a case of such type, at low Reynolds number, were presented in terms of velocity and temperature fields. They found the existence of relatively strong recirculation zones near the baffles. The eddy zones are responsible of local variations in the Nusselts numbers along the baffles and walls.

We know that the primary heat exchanger goal is to efficiently transfer heat from one fluid to another separated, in most practical cases, by solid wall. To increase heat transfer, several approaches have been proposed. We can cite the specific treatment of solid separation surface (roughness, tube winding, vibration, etc.). This transfer can also be improved by creation of longitudinal vortices in the channel. These eddies are produced by introducing one or more transverse barriers (baffle plates) inside the channel. The formation of these vortices downstream of baffles causes recirculation zones capable of rapid and efficient heat transfer between solid walls and fluid flow. It is this approach that we will follow in this study. Indeed, we are interested in this work on the numerical modeling of dynamic and thermal behavior of turbulent forced convection in

horizontal channel where two walls are raised to a high temperature. This channel may contain one or several rectangular inclined baffles.

A special interest is given to the influence of different parameters, such as number and baffle inclination on heat transfer and fluid flow.

## II. MATHEMATICAL FORMULATION

The geometry of the problem is shown schematically in Figure 1. It is a rectangular duct with isothermal horizontal walls, crossed by a stationary turbulent flow. The physical properties are considered to be constants.

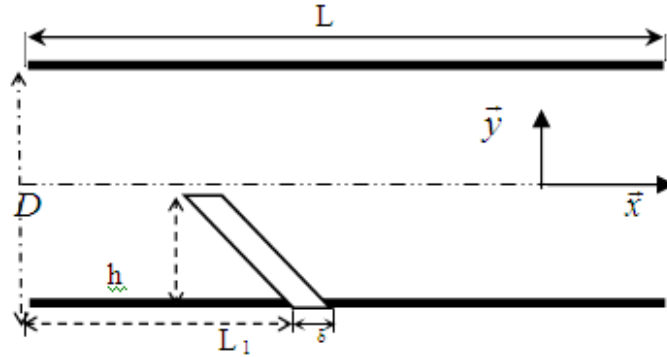


Figure 1: The studied channel

At each point of the flow the velocity has components (u, v) in the x and y directions, and the temperature is denoted T. The turbulence modeling is handled by the classical model (k-ε). k is the turbulent kinetic energy and ε the viscous dissipation of turbulence. The Transport equations (continuity, momentum, temperature, turbulent kinetic energy and dissipation of turbulence) governing the system, are written in the following general form :

$$\frac{\partial(\rho u \phi)}{\partial x} + \frac{\partial(\rho v \phi)}{\partial y} = \frac{\partial \left[ \Gamma_{\phi} \frac{\partial \phi}{\partial x} \right]}{\partial x} + \frac{\partial \left[ \Gamma_{\phi} \frac{\partial \phi}{\partial y} \right]}{\partial y} + S_{\phi} \quad (1)$$

Where ρ is the density of the fluid passing through the channel and φ, Γφ and Sφ are given by:

Equations	φ	Γφ	Sφ
Continuité	1	0	0
Quantité de mouvement selon x	u	μ + μ <sub>t</sub>	$-\frac{\partial P}{\partial x}$
Quantité de mouvement selon y	v	μ + μ <sub>t</sub>	$-\frac{\partial P}{\partial y}$
Energie totale	T	$\mu + \frac{\mu_t}{\sigma_T}$	0
Energie cinétique turbulente	k	$\mu + \frac{\mu_t}{\sigma_k}$	$-\rho \cdot \varepsilon + G$
Dissipation turbulente	ε	$\mu + \frac{\mu_t}{\sigma_{\varepsilon}}$	$(C_1 G - C_2 \rho \varepsilon) \frac{\varepsilon}{k}$

$$G = \mu_t \left\{ 2 \left[ \frac{\partial u}{\partial x} \right]^2 + 2 \left[ \frac{\partial v}{\partial y} \right]^2 + \left[ \frac{\partial v}{\partial x} + \frac{\partial u}{\partial y} \right]^2 \right\}$$

With :

$\mu$  and  $\mu_t$  represent, respectively, the dynamic and turbulent viscosities.

$$\mu_t = \rho \cdot C_\mu \frac{k^2}{\varepsilon}$$

The constants used in the turbulence model (k- $\varepsilon$ ) Are those adopted by Chieng and Launder (1980) [8] :

$C_\mu$	$C_1$	$C_2$	$\sigma_T$	$\sigma_k$	$\sigma_\varepsilon$
0,09	1,44	1,92	0,9	1	1,3

Boundary conditions :

At the channel inlet:

$$u = U_{in} ; v = 0 \text{ and } T = T_{in}$$

$$k = 0,005 U_{in}^2 \text{ and } \varepsilon = 0,1 k^{3/2}$$

At solid walls:

$$u = v = 0 ; k = \varepsilon = 0 \text{ and } T = T_w \succ T_{in}$$

**At the channel exits:**

The gradient of any quantity, with respect to the longitudinal direction x is nul. Our goal is to determine velocity and temperature fields, as well as the turbulence parameters. Particular attention is given to the quantification parameters reflecting heat exchanges such as the Nusselt number (local and average).

### III. NUMERICAL PROCEDURE

The computer code that we have developed is based on a finite volume method. Computational domain is divided into a number of stitches. To choose the number of cells used in this study, we performed several simulations on a channel (with or without baffles). Finally, we have opted for a  $210 \times 90$  meshes. The mesh dimensions are variables; they tighten at the solid walls neighborhoods. Consequently, the stitch density is higher near the hot walls and baffles.

We consider a mesh having dimensions  $\Delta x$  and  $\Delta y$ . In the middle of each volume we consider the points P, called centers of control volumes. E, W, N, S are the centers of the adjacent control volumes. We also consider centers, EE; WW, NN, SS. The faces of each control volume are denoted e, w, n, s 'figure 2'.

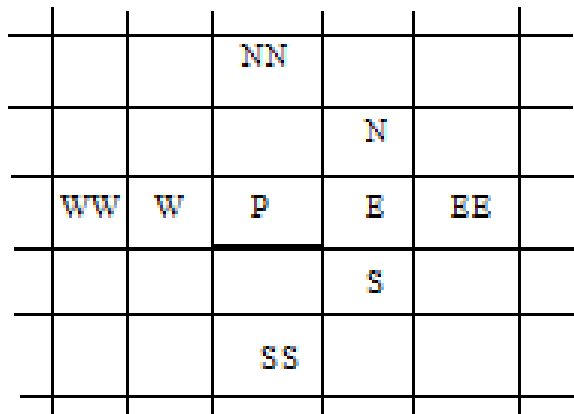


Figure 2: Mesh with P at center

By integrating the transport equation (1) of  $\phi$  on the control volume, we find, a relation to the x direction:

$$[\rho u \phi]_e - [\rho u \phi]_w = \left[ \Gamma \frac{d\phi}{dx} \right]_e - \left[ \Gamma \frac{d\phi}{dx} \right]_w + [S_\phi]_p$$

Where  $[S_\phi]_p$  is the source term.

One note  $F = \rho u$ , the convection flow and  $D = \Gamma / \Delta x$ , the diffusion coefficient. And with taking :

$$F_e = [\rho u]_e ; F_w = [\rho u]_w$$

$$D_e = [\Gamma / \Delta x]_e ; D_w = [\Gamma / \Delta x]_w$$

$$\text{And: } [d\phi]_e = \phi_E - \phi_P \quad ; \quad [d\phi]_w = \phi_P - \phi_W$$

$$\text{We found : } F_e \phi_e - F_w \phi_w = D_e (\phi_E - \phi_P) - D_w (\phi_P - \phi_W) + [S_\phi]_p$$

To estimate  $\phi$  on the faces " e " and " w " we opted for the classical quick scheme [5] which is a quadratic forms using three nodes. The choice of these nodes is dictated by the direction of flow on these faces ( $u > 0$  or  $u < 0$ ).

Finally, the transport equation (1) is discretized on the mesh with P at center as :

$$a_P \phi_P = a_w \phi_w + a_E \phi_E + a_{wW} \phi_{wW} + a_{EE} \phi_{EE} + [S_\phi]_P \quad (2)$$

$$\left\{ \begin{array}{l} a_w = D_w + \frac{6}{8} \alpha_w F_w + \frac{1}{8} \alpha_e F_e + \frac{3}{8} (1 - \alpha_w) F_w \\ a_{wW} = -\frac{1}{8} \alpha_w F_w \\ a_E = D_e - \frac{3}{8} \alpha_e F_e - \frac{6}{8} (1 - \alpha_e) F_e - \frac{1}{8} (1 - \alpha_w) F_w \\ a_{EE} = \frac{1}{8} (1 - \alpha_e) F_e \\ \text{With : } a_P = a_w + a_{wW} + a_E + a_{EE} - [S_\phi]_P \end{array} \right.$$

$$\text{Where: } \alpha_e = 1 \text{ or } 0, \text{ if } F_e > 0 \text{ or } F_e < 0$$

$$\alpha_w = 1 \text{ or } 0, \text{ if } F_w > 0 \text{ or } F_w < 0$$

The same thing is done for the vertical "y" direction, using the faces "n" and "s" and by introducing the Quick diagram nodes N, NN, S and SS.

If convection flow and diffusion coefficient of the sides "e", "w", "s", "n" are known And especially the source term  $[S_\phi]_p$ , the solution of equation (2) then gives us the values of  $\phi$  in different P nodes.

One notes that to accelerate the convergence of equation (2) we have introduced a relaxation factor :

$$\frac{a_P}{\beta} \phi_P = a_w \phi_w + a_E \phi_E + a_{wW} \phi_{wW} + a_{EE} \phi_{EE} + [S_\phi]_P + \frac{1 - \beta}{\beta} a_P \phi_P^0 \quad (3)$$

Where  $\phi_P^0$  is the value of  $\phi_P$  in the previous step.

The source term appears especially in the conservation of momentum equations in the form of a pressure gradient which is in principle unknown. To get around this coupling we have chosen to use in our code the "SIMPLE" algorithm developed by Pantankar [7]. The basic idea of this algorithm is to assume a field of initial pressure and inject it into the equations of conservation of momentum. Then we solve the system to find a field of intermediate speed (which is not fair because the pressure isn't.) The continuity equation is transformed into a pressure correction equation. This last is determined to find a pressure correction that will inject a new pressure in the equations of motion. The cycle is repeated as many times as necessary until a pressure correction

equal "zero" corresponding to the algorithm convergence. In the end we solve the transport equations of  $T$ ,  $k$  and  $\mathcal{E}$ . In this approach, a problem is encountered. It is known as the checkerboard problem.

The risk is that a pressure field can be highly disturbed by the sensed formulation which comprises performing a linear interpolation for estimate the pressure value on the facets of the control volume. To circumvent this problem we use the so-called staggered grids proposed by Harlow and Welch [6]. In this technique, a first grid pressure (and other scalar quantities  $T$ ,  $k$  and  $\mathcal{E}$ ) is placed in the center of the control volume. While other staggered grids are adopted for the velocity components  $u$  and  $v$  (see Figure 3).

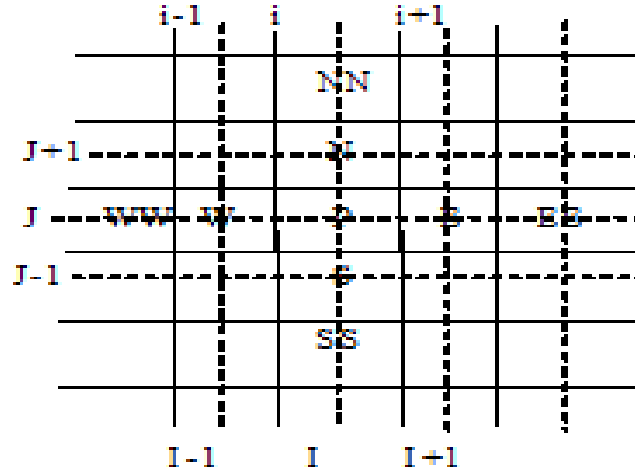


Figure 3: Shifted mesh

The scalar variables, including pressure, are stored at the nodes  $(I, J)$ . Each node  $(I, J)$  is surrounded by nodes  $E, W, S$  and  $N$ . The horizontal velocity component  $u$  is stored on faces "e" and "w", while the vertical component  $v$  is stored on the faces denoted "n" and "s".

So the control volume for pressure and other scalar quantities  $T, k$  and  $\mathcal{E}$  is

$$[(i + 1, j); (i + 1, j + 1); (i, j + 1); (i, j)]$$

For component  $u$  control volume is

$$[(I, j); (I, j + 1); (I - 1, j + 1); (I - 1, j)]$$

While for the  $v$  component we use:  $[(i + 1, J - 1); (i + 1, J); (i, J); (i - 1, J - 1)]$ .

By integrating the conservation momentum equation in the horizontal direction on the volume  $[(I, j); (I, j + 1); (I - 1, j + 1); (I - 1, j)]$ , we found :

$$a_{i,j} u_{i,j} = \sum a_{nb} u_{nb} + [P(I - 1, J) - P(I, J)](y_{j+1} - y_j) \quad (4)$$

$$\text{Where: } \sum a_{nb} u_{nb} = a_{ww} u_{ww} + a_w u_w + a_{ee} u_{ee} + a_e u_e + a_{ss} u_{ss} + a_s u_s + a_{nn} u_{nn} + a_n u_n$$

The coefficients  $a_{nb}$  are determined by the quick scheme mentioned above.

Similarly, the integration of conservation momentum equation in the vertical direction on the volume

$$[(i + 1, J - 1); (i + 1, J); (i, J); (i - 1, J - 1)], \text{ gives:}$$

$$a_{I,j} v_{I,j} = \sum a_{nb} v_{nb} + [P(I, J - 1) - P(I, J)](x_{i+1} - x_i) \quad (5)$$

One considers primarily an initial pressure field  $P^*$ . The provisional solution of the equations (4) and (5) will be denoted  $u^*$  and  $v^*$ . We note that  $u^*$  and  $v^*$  doesn't checks the continuity equation, and:

$$a_{i,j} u^*_{i,j} = \sum a_{nb} u^*_{nb} + [P^*(I - 1, J) - P^*(I, J)](y_{j+1} - y_j) \quad (6-a)$$

$$a_{I,j} v^*_{I,j} = \sum a_{nb} v^*_{nb} + [P^*(I, J - 1) - P^*(I, J)](x_{i+1} - x_i) \quad (6-b)$$

At this stage any one of the three variables is correct, they require correction :

$$\begin{cases} p' = P - P^* \\ u' = u - u^* \\ v' = v - v^* \end{cases} \quad (7)$$

Injecting (7) in equations (4), (5) and (6) we find :

$$a_{i,j} u'_{i,j} = \sum a_{nb} u'_{nb} + [P'(I-1, J) - P'(I, J)](y_{j+1} - y_j) \quad (8-a)$$

$$a_{i,j} v'_{i,j} = \sum a_{nb} v'_{nb} + [P'(I, J-1) - P'(I, J)](x_{i+1} - x_i) \quad (8-b)$$

At this level, an approximation is introduced. In order to linearize the equations (8), the terms

$$\sum a_{nb} u'_{nb} \quad \text{and} \quad \sum a_{nb} v'_{nb}$$

are simply neglected. Normally these terms must cancel at the procedure convergence. That is to say that this omission does not affect the final result. However, the convergence rate is changed by this simplification. It turns out that the correction P' is overestimated by the Simple algorithm and the calculation tends to diverge. The remedy to stabilize the calculations is to use a relaxation factor.

We Note that a further treatment of these terms is proposed in the so-called algorithms "SIMPLER" and "SIMPLEC" [7].

The equations (8) become :

$$u'_{i,j} = d_{i,j} [P'(I-1, J) - P'(I, J)] \quad (9-a)$$

$$v'_{i,j} = d_{i,j} [P'(I, J-1) - P'(I, J)] \quad (9-b)$$

$$d_{i,j} = \frac{y_{j+1} - y_j}{a_{i,j}} \quad \text{and} \quad d_{i,j} = \frac{x_{i+1} - x_i}{a_{i,j}}$$

With :

Equations (9) give the corrections to apply on velocities through the formulas (7). We have therefore :

$$u_{i,j} = u^*_{i,j} + d_{i,j} [P'(I-1, J) - P'(I, J)] \quad (10-a)$$

$$v_{i,j} = v^*_{i,j} + d_{i,j} [P'(I, J-1) - P'(I, J)] \quad (10-b)$$

Now the discretized continuity equation on the control volume of scalar quantities is written as follows :

$$[(\rho u A)_{i+1,j} - (\rho u A)_{i,j}] - [(\rho v A)_{i,j+1} - (\rho v A)_{i,j}] = 0$$

Where A are the size of the corresponding faces.

The introduction of the velocity correction equations (10) in the continuity equation gives a final equation allowing us to determine the scope of pressure corrections P':

$$a'_{i,j} P'(I, J) = a'_{i+1,j} P'(I+1, J) + a'_{i-1,j} P'(I-1, J) + a'_{i,j+1} P'(I, J+1) + a'_{i,j-1} P'(I, J-1) \quad (11)$$

The algorithm can be summarized as follows : one starts from an initial field  $P^*, u^*, v^*$  and  $\phi^*$ , with  $\phi$  represents the scalar quantities T, k and  $\mathcal{E}$ . Then the system (6) is solved to have new values of  $u^*$  and  $v^*$ .

Then the system (11) is solved for the corrections field pressure P'.

Thereafter, pressure and velocity are corrected by equations (7) and (10) to have P, u and v.

We solve the following transport equation of scalar quantities (2),  $\phi = T, K$  and  $\mathcal{E}$ .

Finally, we consider:  $P^* = P ; u^* = u ; v^* = v ; \phi^* = \phi$ .

and the cycle is repeated until convergence.

#### IV. RESULTS AND DISCUSSIONS

The dimensions of the channel presented in this work are based on experimental data published by Demartini et al [2]. The air flow is carried out under the following conditions.

- channel length:  $L = 0.554 \text{ m}$ ;
- channel diameter  $D = 0.146 \text{ m}$ ;
- baffle height :  $h = 0.1 \text{ m}$ ;
- Baffle thickness:  $\delta = 0.01 \text{ m}$  ;
- Reynolds number:  $Re = 8.73 \cdot 10^4$ ;

The hydrodynamic and thermal boundary conditions are given by :

At the channel inlet:

$$u = u_{in} = 7.8 \text{ m/s}; \quad \mathbf{V} = 0; \quad T = T_{in} = 300 \text{ }^\circ\text{K}$$

On the channel walls:

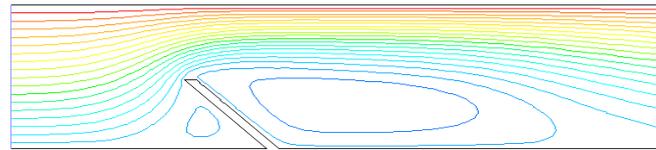
$$u = v = 0 \quad \text{and} \quad T = T_w = 373 \text{ }^\circ\text{K}$$

At the channel exit the system is assumed to be fully developed:

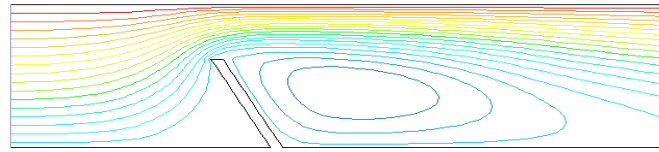
$$\frac{\partial u}{\partial x} = \frac{\partial v}{\partial x} = \frac{\partial T}{\partial x} = 0$$

First, we compared the structure of streamlines and isotherms in channels with baffles having different inclination angles. Baffle is located at the abscise  $L_1 = 0.218 \text{ m}$ . Indeed, in figures 4 and 5 we present streamlines and isotherms for three values of inclination angle.

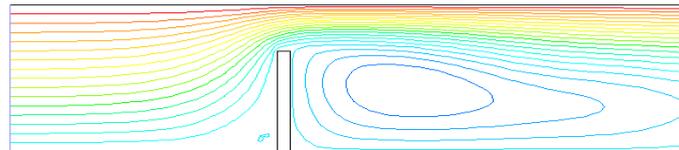
These results clearly show the importance of presence of baffle (acting as a cooling fin) [9]. Since the recirculation zone, downstream of the baffle, depend on the inclination angle so this last affect isotherms and streamlines structures and affect, consequently, the heat transfer through the channel. Indeed the baffle increases heat transfer between the wall and the fluid. So this increase depends on baffle position [9] and angle inclination.



Case 1-1  $\alpha = 45^\circ$

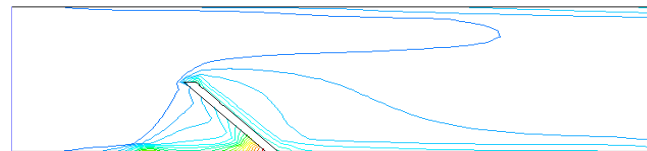


(b) Case 1-2  $\alpha = 60^\circ$

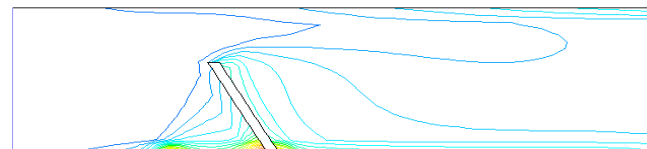


(c) Case 1-3  $\alpha = 90^\circ$

Figure 4: streamlines



Case 1-1  $\alpha = 45^\circ$



Case 1-2  $\alpha = 60^\circ$

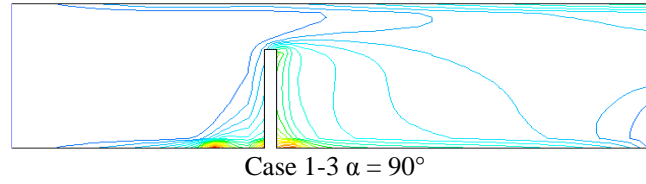


figure 5: Isotherms 'one baffle'

It is clear that the isotherms are more condensed near baffle, top and bottom walls when the inclination angle  $\alpha$  increases. This indicates an increase of heat transfer near baffle. Indeed, the increase in  $\alpha$  expanded exchange area between fluid and walls. This is because the flow is blocked by the baffle when  $\alpha$  is small. In addition, when  $\alpha$  increases, the recirculation zone becomes increasingly important (see Figure 4). This causes an acceleration of turbulent flow in this region, which improves heat transfer within the channel.

We present figures 6 and 7 in order to identify the influence of  $\alpha$  on velocities and temperature profiles along  $y$  at  $x = 0.45$  m ; from channel inlet.

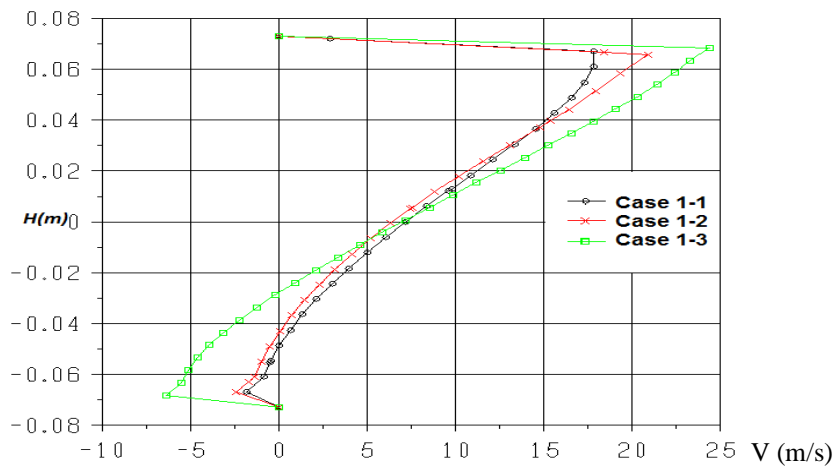


Figure 6: Horizontal velocity Profiles along  $y$  at  $x = 0.45$  m « influence of  $\alpha$  »

These results allow us to conclude that the effect of baffle inclination on temperature profile and velocity distribution depend on channel regions 'bottom and top'. Indeed, the velocity is maximal in the top half channel when  $\alpha$  is maximal and the inverse is true in the bottom half channel.

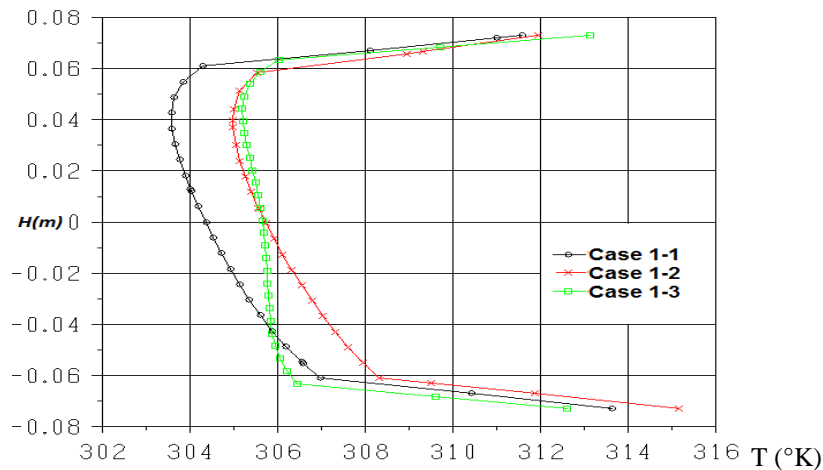


Figure 7: Temperature profiles along  $y$  at  $x = 0.45$  m « influence of  $\alpha$  »

Concerning temperature profiles at  $x = 0.45$  m, we can see that there are similar between cases 1-1 and 1-2, with a nearly constant difference. However, the temperature is maximal for cases 1-1 and minimal for cases 1-2.

In the purpose of measuring the influence of ' $\alpha$ ' on local heat transfer, we have presented in figure 8, the local Nusselt number along the channel for the considered cases.

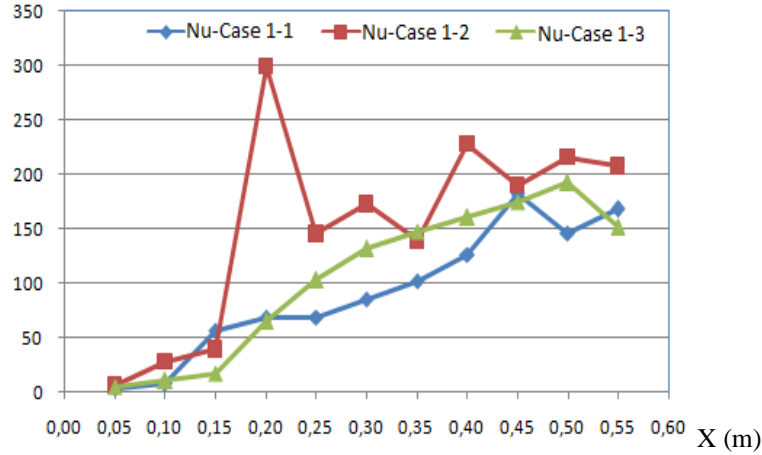
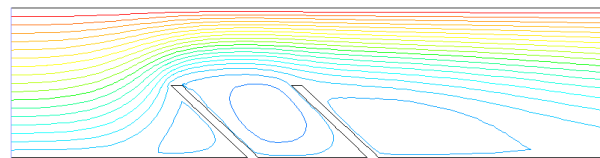
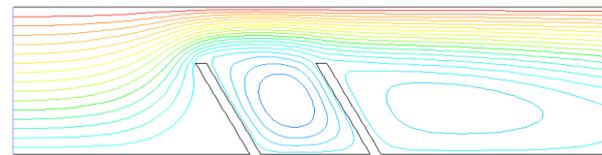


Figure 8 : Local Nusselt number along the channel « influence of  $\alpha$  »

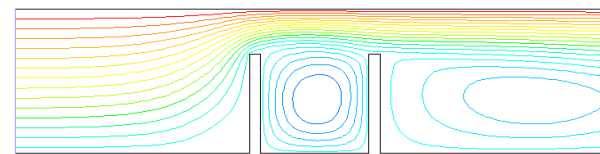
It shows that upstream of the baffle ( $x < 0.15$  m) curves are confused, while, just after this location, effect of baffle inclination on Nusselt number become increasingly important away from baffles. Indeed, the local Nusselt number in the case 1-1 is more important than the other cases. This indicates that heat transfer is higher in the case 1-1.



Case 2-1:  $\alpha = 45^\circ$



Case 2-2:  $\alpha = 60^\circ$



Case 2-3:  $\alpha = 90^\circ$

Figure 9 : Streamlines 'two baffles'

We consider two baffles of same height  $h = 0.1$  m. The first baffle is placed at the distance  $L_1 = 0.15$  m, while the second is positioned at the distance  $d_1 = 0.10$  m from the first. In order to investigate the inclination angle we have chosen three different inclination angles;  $\alpha = 45^\circ$  (case 2-1),  $\alpha = 60^\circ$  (case 2-2) and  $\alpha = 90^\circ$  (case 2-3). We note the existence of two recirculation zones downstream of the first baffle. Also the first recirculation zone delimited by baffles becomes increasingly important with increasing  $\alpha$ , which contribute to an increase in heat transfer in this area, as shown in Figure 10. Indeed, when the baffles are vertical  $\alpha = 90^\circ$ , the fluid is blocked in the chimney delimited by two baffles. Which reduces the flow speed at that location and thus

there will be a decrease in the heat transfer in this area. In addition, when  $\alpha$  increase, the fluid has sufficient space to move rapidly, hence heat transfer increases in this zone 'see figure13'.

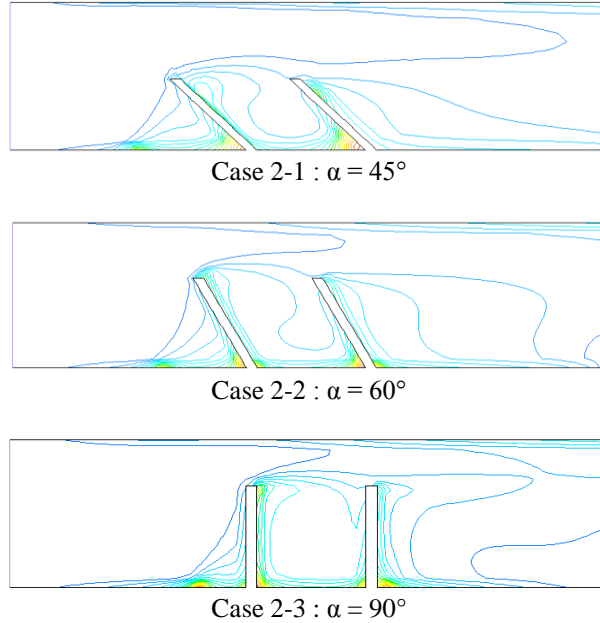


Figure 10 : Isotherms 'two baffles'

In the following figures 11 and 12, we compare the profile of horizontal velocity and temperature distribution. Calculation is done on the y-axis at  $x = 0.45$  m from the channel inlet for three different baffles inclination angles. We can distinguish two zones, the first defined by  $0.02 < Y < 0.08$  and the second by  $0.08 < Y < 0.02$ . In the first zone, we note that the increase of  $\alpha$  contribute to an increase in the horizontal flow velocity; whereas, there is an opposite effect for the second region.

Concerning temperature distribution at  $x = 0.45$  m, one distinguish two different zones: in the top region, corresponding to the interval  $0.02 < Y < 0.08$ , fluid temperature is higher in the case of vertical baffles ' $\alpha = 90^\circ$ '. Whereas it's lower in the bottom region, corresponding to  $-0.08 < Y < 0$ . This can be explained by the fact that the fluid passing the region between the first baffle and the channel top wall is heated more and more when the inclination angle,  $\alpha$ , increases. This is because this region becomes small as the inclination angle  $\alpha$  increases. Thereby the fluid reaches the second baffle with a higher temperature and velocity. Indeed the higher velocity allows the fluid to keep its temperature, due to the exchange with the lower cold region minimal. Consequently the fluid in the lower region has a minimal temperature.

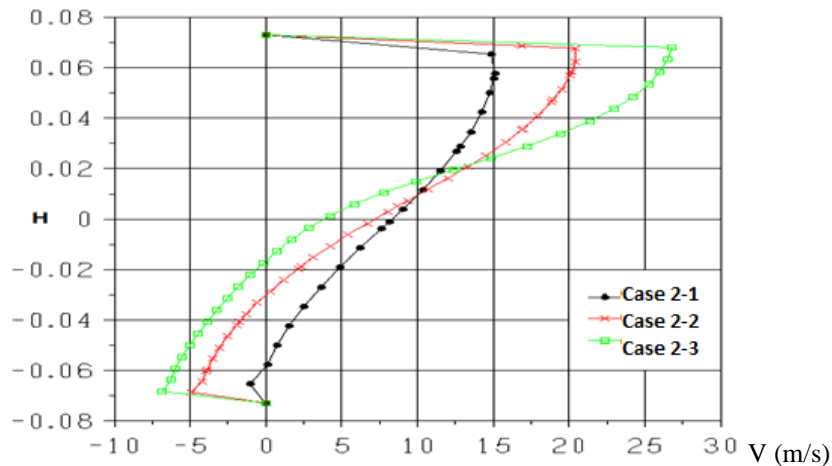


Figure 11: Profiles of the horizontal velocity at  $x = 0.45$  m « influence of  $\alpha$  »

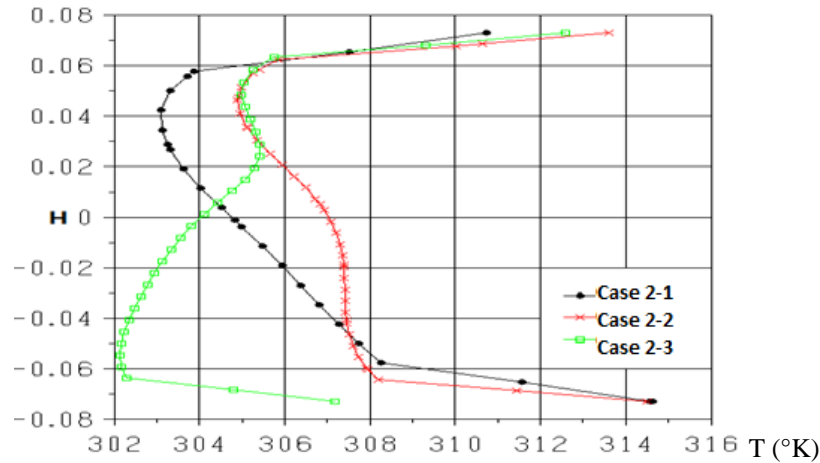


Figure 12: Profiles of the total temperature at  $x = 0.45$  m « influence of  $\alpha$  »

Figure 13 present the local Nusselt number along the channel for three considered inclination angles.

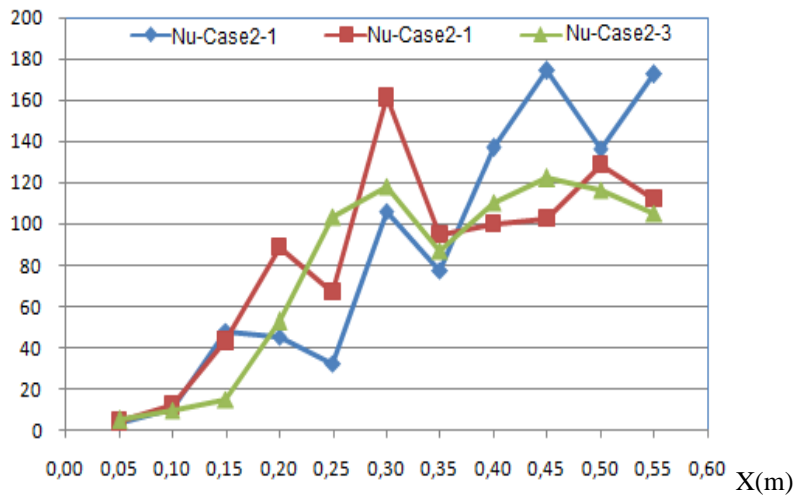


Figure 13: Local Nusselt number along the channel « Influence of  $\alpha$  »

Since the local Nusselt number shows the local heat transfer by convection, because it has a relation with the velocity and temperature distribution, its structure depend on the latter. Indeed, we distingue different zones. The first defined by  $0 < x < 0.35$  m while the second by  $x > 0.35$  m. For the first region, the local nusselt number is higher for  $\alpha = 60^\circ$  and lower for  $\alpha = 45^\circ$  which means that the heat transfer is important in the first case and lower in the second case; whereas the reverse is true for the second zone. One note that the heat transfer is maximal for  $\alpha = 45^\circ$  and minimal for  $\alpha = 60^\circ$ . Let's note that local nusselt number for every case present two 'peaks' corresponding to baffles positions.

We chooses to show the influence of baffles number on heat transfer along the channel for vertical baffles 'inclination angle  $\alpha = 90^\circ$ '. We have chosen to show case 1-3 'channel having single baffle' and case 2-3 'channel containing two baffles', see figure 14. It should be noted that generally, heat transfer is inversely proportional to baffles number. Indeed, the Nusselt number characterizing heat transfer within the channel decrease with increasing baffles number.

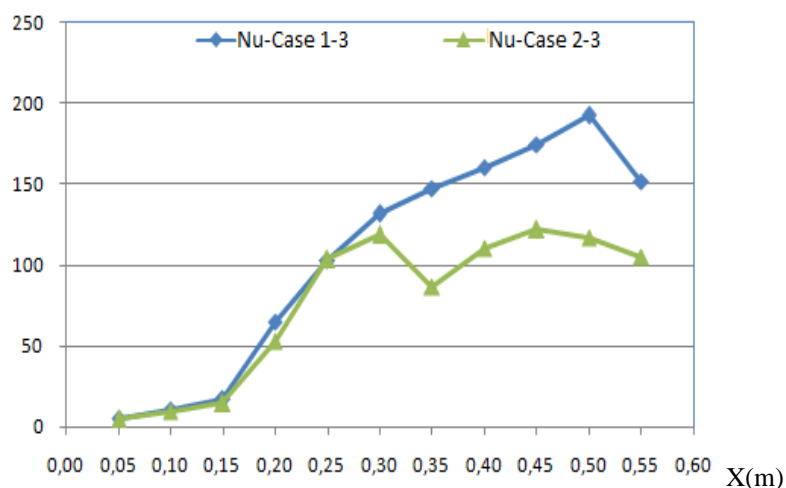


Figure 14: Local Nusselt number along the channel 'influence of baffle number'

## V. CONCLUSION

The thermal behavior of a stationary turbulent forced convection flow within a baffled channel was analyzed. The results show the ability of our code to predict dynamic and thermal fields in various geometric situations. We studied mainly the influence of baffles inclination and number on heat transfer and fluid flow. One can conclude that the increase in the baffle inclination improves heat transfer between channel walls and fluid passing through it; and that heat transfer becomes decreasingly important with adding baffles.

In perspective, we intend deepen and clarify our results. Indeed, we will adapt our code to others geometric cases (non-rectangular baffles or baffles). Finally, we will also try to refine more the turbulence model.

## REFERENCES

- [1]. S.V.PATANKAR, E.M.SPARRROW, « Fully developed flow and heat transfer in ducts having stream wise-periodic variations of cross-sectional area », Journal of Heat Transfer, Vol. 99, p (180-6), 1977.
- [2]. L.C.DEMARTNI, H.A.VIELMO and S.V.MOLLER, « Numerical and experimental analysis of the turbulent flow through a channel with baffle plates », J. of the Braz. Soc. of Mech. Sci. & Eng., Vol. XXVI, No. 2, p (153-159), 2004.
- [3]. R.SAIM, S.ABBOUDI, B.BENYOUCEF, A.AZZI, « Simulation numérique de la convection forcée turbulente dans les échangeurs de chaleur à faisceau et calandre munis des chicanes transversales », Algérien journal of applied fluid mechanics / vol 2 / 2007 (ISSN 1718 – 5130).
- [4]. M. H. NASIRUDDIN, K. SEDDIQUI « Heat transfert augmentation in a heat exchanger tube using a baffle», International journal of Heat and Fluid Flow, 28 (2007), 318-328.
- [5]. H.K. Versteeg ; W. Malalasekera « An introduction to computational fluid dynamics » ISBN 0.582-21884-5.
- [6]. F. Harlow; J. Welsh ; « Staggered grid », Numerical calculation of time dependent viscous incompressible flow with free surface. Physics of fluids, vol. 8; pp 2182-2189; 1965.
- [7]. Patankar, S.V. (1980), «Numerical Heat Transfer and Fluid Flow», Hemisphere/McGraw-Hill, New York, NY.
- [8]. Chieng C.C. and Launder B.E. «On the calculation of turbulent heat transport downstream from an abrupt pipe expansion», Numerical Heat Transfer, vol. 3, pp. 189-207.
- [9]. M.A. Louhibi, N. Salhi, H. Bouali and S. Louhibi «Numerical modeling of heat transfer in an channel with transverse baffles» International Journal of Engineering Research and Development, e-ISSN: 2278-067X, P-ISSN: 2278-800X, Vol. 8, Issue 12, PP. 06-18.